



## Detecting Bifurcations from Time Series Data

Kazuto OGOSHI, Hiroyuki KITAJIMA and Toru YAZAWA

†Faculty of Engineering, Kagawa University  
2217-20 Hayashi, Takamatsu, Kagawa 761-0396, Japan  
Email: s16g454@stu.kagawa-u.ac.jp, {kitaji,tyazawa}@eng.kagawa-u.ac.jp

**Abstract**—In this paper, we try to detect the early-warning signal from time series data. Simple mathematical models with noise and a real system are used to obtain the data. We calculate autocorrelation functions at the parameter values close to and away from a bifurcation. We determine that an averaged peak interval of the autocorrelation function is a good indicator for predicting bifurcations.

### 1. Introduction

Detecting bifurcation points from time series is the important and challenging issue because complex dynamical systems, ranging from ecosystems to financial markets and the climate, can have critical points at which a sudden shift to a contrasting dynamical regime may occur [1, 2, 3]. Scheffer et al. reviewed many methods of detecting early-warning signals applied to simple mathematical models to real systems [1]. Chen et al. detected a “pre-disease” state using network biomarkers [4]. Peng et al. proposed detrended fluctuation analysis (DFA) for determining the statistical self-affinity of a signal [5] and applied it to heartbeat time series data [6]. Yazawa proposed a modified DFA method and obtained a scaling index of judging a healthy condition from heartbeat [7].

In this study, we use the autocorrelation function (ACF) to capture early-warning signals just before bifurcations in simple mathematical models. Then, we apply it to heartbeat data from an experiment. We determine that the averaged peak interval of the autocorrelation function is one of good indicators for detecting bifurcations.

### 2. Model equations

We use the BVP model [8] and Luo-Rudy model [9] in this study. BVP equations are described by

$$\begin{aligned} \frac{dx}{dt} &= \omega y - \sigma x \\ \frac{dy}{dt} &= -\omega x + \epsilon(1 - \beta y^2)y. \end{aligned} \quad (1)$$

These equations describe the behavior of an electric circuit containing an inductor, a capacitor, and linear and non-linear resistors [8]. These equations are derived from the simplification of the Hodgkin-Huxley equations which describe the electric property of the squid axon. In this paper,

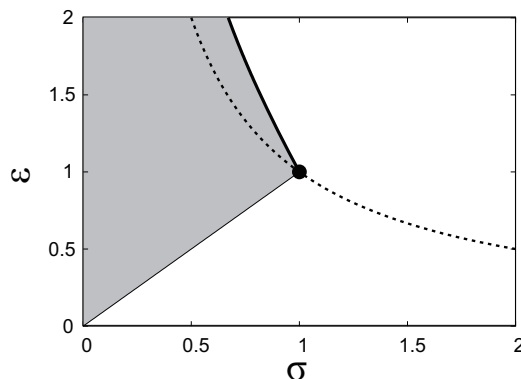


Figure 1: Bifurcation diagram for BVP equations

we set  $\omega = 1.0$  and  $\beta = 1.0$ , and change the values of  $\epsilon$  and  $\sigma$ .

The membrane potential  $V$  of the LR model with the synaptic external input is described by

$$C \frac{dV}{dt} = -(I_{Na} + I_{Ca} + I_K + I_{K1} + I_{Kp} + I_b + I_{syn}). \quad (2)$$

This is a mathematical model of the mammalian (guinea pig) ventricular cell. In this paper, we change the values of  $[K]_o$  (free concentration of the potassium ions in the extracellular compartment) because we had determined that increasing  $[K]_o$  triggers a period-doubling bifurcation generating alternans [10].

### 3. Results

#### 3.1. BVP model

A bifurcation diagram is shown in Fig. 1. In this figure, thin solid and dotted curves indicate Hopf and pitchfork bifurcations of equilibrium points, respectively. A periodic solution is generated by crossing the Hopf bifurcation from bottom to up. The periodic solution disappears by the tangent bifurcation denoted by a thick solid curve in Fig. 1. We observe the stable periodic solution in a gray parameter region. Here, we try to quantify the stability of the periodic solution from time series of the state variable  $x$ . We set  $\epsilon = 2.0$  and change the value of  $\sigma$  in Eq. (1) to control the distance to the tangent bifurcation.

Figures 2(a) and 2(b) show waveforms of  $x$  at the points away from and close to the bifurcation point. Next, we

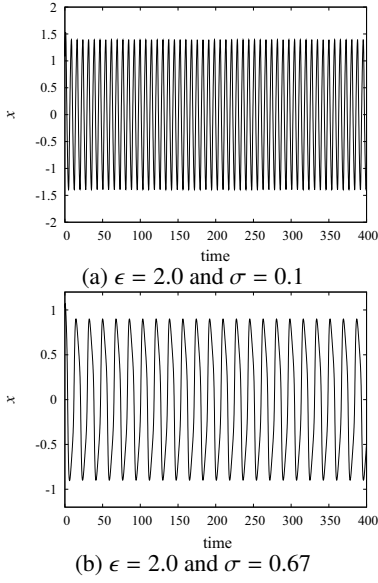


Figure 2: Waveforms of  $x$

add the Gaussian white noise  $\xi_i(t)$  to  $x$  in Eq. (1), where  $\langle \xi_i(t) \xi_i(t') \rangle = \delta(t - t')$ . Noise-added waveforms of  $x$  are shown in Figs. 3(a) and 3(b). We calculate ACFs for Figs. 3(a) and 3(b). The ACF of data  $X_i$  is given by

$$R(\tau) = \frac{E[(X_i - \mu)(X_{i+\tau} - \mu)]}{\eta^2} \quad (3)$$

where  $E[\cdot]$  is the expected value,  $\mu$  and  $\eta$  are the mean and variance of data  $X_i$ , respectively. The results are shown in Figs. 4(a) and 4(b). Next, we calculate the mean of peak

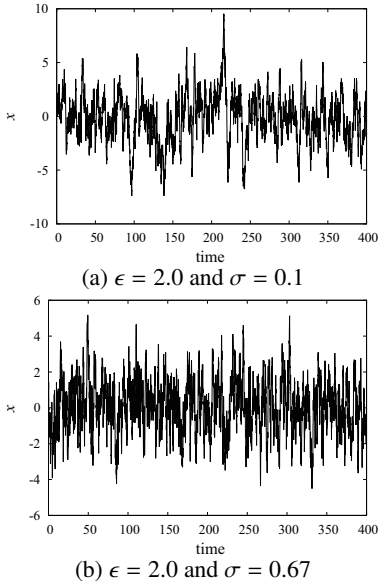


Figure 3: Noise-added waveforms of  $x$

intervals of low-passed noise-added waveforms as a function of the parameter  $\sigma$  to estimate the stability of the periodic solution. The result is shown by a solid curve in Fig. 5.

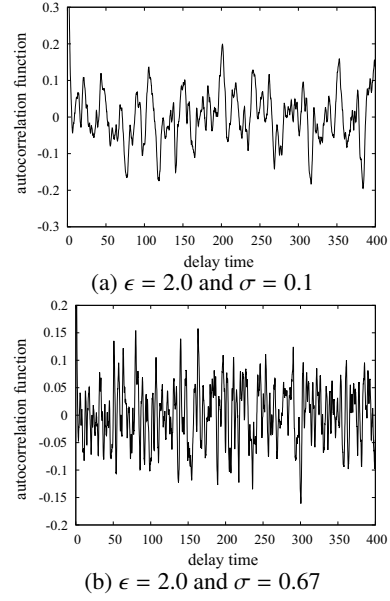


Figure 4: Autocorrelation function of noise-added waveforms

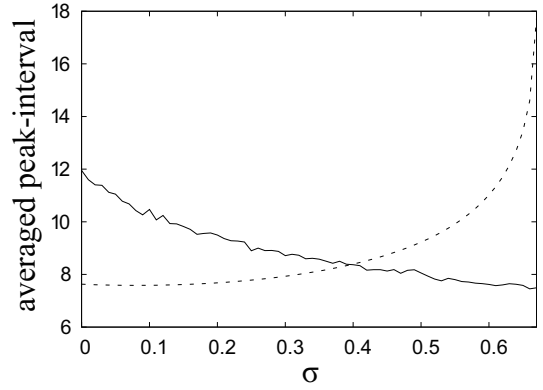


Figure 5: Period of periodic solution (dotted curve) and mean of peak intervals of noise-added waveform (solid curve) as a function of  $\sigma$

Note that the tangent bifurcation occurs at  $\sigma \approx 0.6711$ . We also present the period of the periodic solution in the noise-free system for comparison (a dotted curve in Fig. 5). The period of the noise-free data is increased as  $\sigma$  approaches the bifurcation point. On the other hand, the averaged peak intervals are decreased. We consider that this characteristic of the averaged peak intervals is independent of the nature of the periodic solution in the noise-free system, thus the averaged peak interval of the ACF is one candidate for detecting a bifurcation point from time series data.

### 3.2. Luo-Rudy model

Next, we apply our indicator to the Luo-Rudy model. We try to quantify the stability of the periodic solution from time series of the membrane potential  $V$ . We change the

values of  $[K]_o$ : a normal value in [9] is 5.4 and a period-doubling bifurcation occurs around 6.583 [10]. Figures 6(a) and 6(b) show waveforms of  $V$  at these parameter values. Next, we add the Gaussian white noise to  $V$  in Eq. (2). We add the noise during phase 2 (plateaus of  $V$ ). Resultant waveforms are shown in Figs. 7(a) and 7(b). We calculate ACFs for these waveforms, which are shown in Figs. 8(a) and 8(b). A two-periodic-like waveform of the ACF appears only in Fig. 8(b), thus the ACF has a possibility of discrimination between Figs. 6(a) and 6(b).

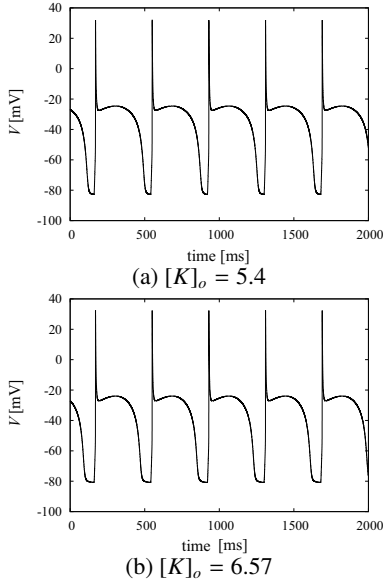


Figure 6: Waveforms of  $V$  in Luo-Rudy model

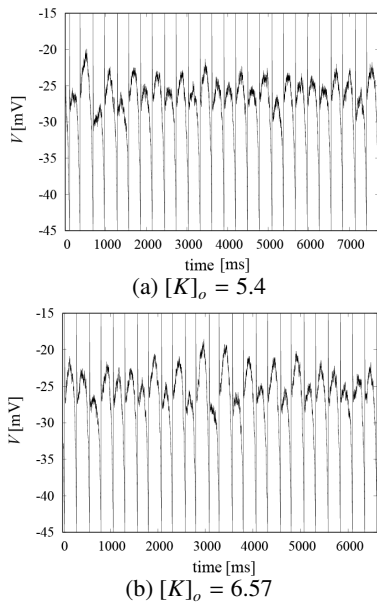


Figure 7: Noise-added waveforms for Luo-Rudy model

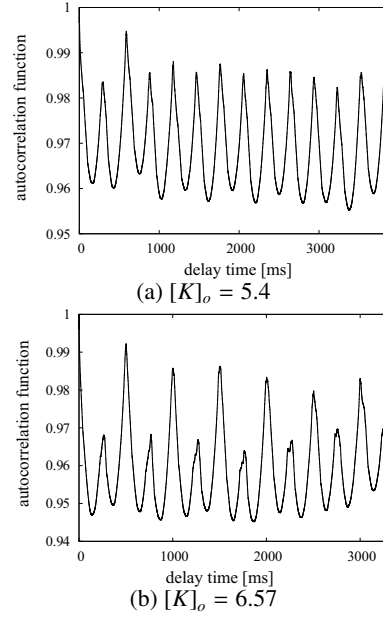


Figure 8: ACF for Luo-Rudy

### 3.3. Experimental data

Next, we apply our indicator to a real system. Yazawa measured the heartbeat of bumblebees for a long time. Figures 9(a) and 9(b) show typical waveforms of a normal state and just before generating abnormal rhythm. We apply the previous process except for adding noise to these data because these measured data already contain noise. Figures 10(a) and 10(b) show ACFs of Figs. 9(a) and 9(b). The results of the averaged peak intervals are 143.999[ms] and 219.857[ms] for a normal state and just before an abnormal state, respectively. The indicator is increased as the state approaches a abnormal state. It is an opposite result to the BVP model. The detailed analysis is one of our future problems.

### 4. Conclusion

We investigated indicators of detecting bifurcation points from time series in mathematical models and experimental data. First, we determined that the averaged peak interval of the autocorrelation function is one of good indicators for detecting a tangent bifurcation using the BVP model. Second, we applied our indicator to more realistic mathematical model: a model of the mammalian (guinea pig) ventricular cell. The autocorrelation function between a normal state and just before a period-doubling bifurcation have different shapes, however the averaged peak interval of the autocorrelation function is almost the same because the period of the external input is the same. We are now trying to quantify these differences. Last, we applied it to experimental data on heartbeat of bumblebees. However, the result is opposite to the BVP's case. We need more results for various computer simulations and experimental

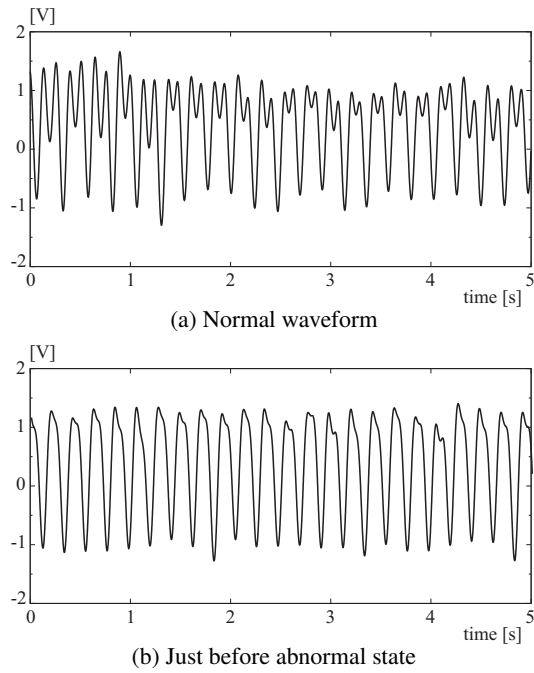


Figure 9: Heartbeat of bumblebee

data to check the validity of our method. Now we are tackling such issues to obtain better results.

### Acknowledgments

This work was supported by JSPS KAKENHI Grant Number 15K00405.

### References

- [1] M. Scheffer et al., Early-warning signals for critical transitions, *Nature*, 461, pp.53-59, 2009.
- [2] M. S. Williamson and T. M. Lenton, Detection of bifurcations in noisy coupled systems from multiple time series, *Chaos*, 25(3), 036407, 2015.
- [3] L. Glass, L, Dynamical disease: Challenges for non-linear dynamics and medicine. *Chaos*, 25(9), 097603, 2015.
- [4] L. Chen, R. Liu, Z. P. Liu, M. Li and K. Aihara, Detecting early-warning signals for sudden deterioration of complex diseases by dynamical network biomarkers, *Scientific Reports*, 2, 342, 2012.
- [5] C. K. Peng, S. V. Buldyrev, S. Havlin, M. Simons, H. E. Stanley and A. L. Goldberger, Mosaic organization of DNA nucleotides, *Physical Review E*, 49(2), 1685, 1994.
- [6] C. K. Peng, S. Havlin, H. E. Stanley and A. L. Goldberger, Quantification of scaling exponents and

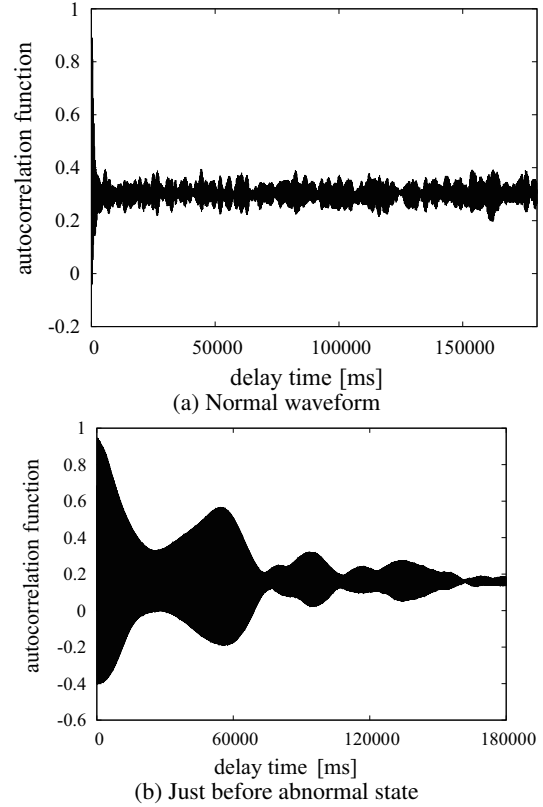


Figure 10: ACF for heartbeat of bumblebee

crossover phenomena in nonstationary heartbeat time series, *Chaos*, 5(1), 82–87, 1995.

- [7] T. Yazawa, *Modified Detrended Fluctuation Analysis (mDFA)*, ASME, New York, 2015.
- [8] R. Fitzhugh, Impulses and physiological states in theoretical models of nerve membrane, *Biophysical Journal*, 1(6), pp.445-466, 1961.
- [9] C.H. Luo and Y. Rudy, A model of the ventricular cardiac action potential. Demoralization, repolarization, and their interaction, *Circ. Res.*, 68, 1501–1526, 1991.
- [10] H. Kitajima, E. Ioka and T. Yazawa, Generation mechanism of alternans in Luo-Rudy model, *Int. J. Bifurcation and Chaos*, 26(5), 1650075, 2016.